Hydrogen Liquefaction by Magnetic Refrigeration

K. Kamiya[1], H. Takahashi[2], T. Numazawa[1],
H. Nozawa[3], and T. Yanagitani[3]

[1]National Institute for Materials Science
 Ibaraki 305-0003 Japan
[2]Chiba University
 Chiba 263-8522 Japan
[3]Konoshima Chemical Co. Ltd
 Kagawa 769-1103 Japan

ABSTRACT

This paper describes a new method of hydrogen liquefaction with a newly developed magnetic refrigerator. Magnetic refrigeration makes use of the magnetocaloric effect, and is well known as an efficient method, in principal, because its cooling cycle can closely follow the Carnot cycle with appropriate heat switches. A liquefaction principle of our magnetic refrigerator is based on a thermo-siphon method, in which liquid hydrogen is condensed directly onto the surface of magnetic refrigerants and drops downward. Therefore, the magnetic refrigerants are required to have relatively large entropy change at liquefaction temperature of hydrogen and hydrogen resistance. Since most metal compounds don't satisfy the latter condition, we have developed a new ceramic polycrystal magnetic refrigerant named dysprosium gadolinium aluminum garnet (DGAG). In the liquefaction experiments, we have successfully liquefied hydrogen gas preliminarily cooled to a temperature slightly above the boiling point. Liquefaction was confirmed by the temperature variation of the DGAG, and the resultant condensation efficiency was found to approach 90% of the Carnot efficiency. The maximum cooling power was 14.6 W.

INTRODUCTION

In late years, importance of hydrogen energy for a fuel cell society is ever-increasing. The technology for a hydrogen infrastructure consists of the preparation, the transportation, the storage and the utilization of hydrogen. For transportation, it is desirable for hydrogen to be in a liquid form from the viewpoint of transport efficiency, and a great effort has been made on hydrogen liquefaction method.[1,2] Compared to conventional and existing liquefaction systems using a Joule-Thomson (J-T) valve, magnetic refrigeration for hydrogen liquefaction has a great potential.[3] One of the greatest advantages of magnetic refrigeration is that its cooling cycle can closely follow the Carnot cycle.

In consideration of these circumstances, we have developed a new magnetic refrigerator to liquefy hydrogen. Magnetic refrigeration is a method which makes use of the magnetocaloric effect. This effect causes magnetic materials to become warm by magnetizing and to cool by demagnetizing the applied magnetic field. A basic idea of the magnetocaloric effect is widely known to create ultra-cold temperatures

below 1 K.[4,5] Recently, followed by progress on the performance of magnetocaloric materials, and the invention of a new cooling cycle, the magnetic refrigeration is achieving its practical use in the higher temperature region.[6-12]

Liquefaction study by magnetic refrigeration was first demonstrated by Numazawa using helium, and the efficiency was found to reach 50% Carnot.[3] In succeeding years, Ohira developed a magnetic refrigerator which operated at 20 K, hydrogen liquefaction temperature, and obtained a cooling power of 0.21 W.[13] These magnetic refrigerators are called static refrigerators because the magnetic refrigerant is motionless. The magnetic field applied to the refrigerant is varied by sweeping the current in a superconducting magnet. Since the typical sweep rate of the superconducting magnet is 10mT/sec, 1 cooling cycle takes 1600 sec ($6.25*10^{-4}$ Hz) in the case of 8T operation to result in poor cooling power. In this study, in order to increase the cooling power, the magnetic field applied on the refrigerant is controlled by moving the magnetic refrigerant. In this manner, cooling cycle frequency was found to increase up to 0.5 Hz. It was also shown in the previous calculation that a cooling cycle simulation applied to our magnetic refrigerator gives considerably high efficiency even in the high frequency operation.[14]

HYDROGEN LIQUEFACTION

Liquefaction Principle

Our hydrogen magnetic refrigerator is premised on using hydrogen gas cooled to a temperature slightly above the liquefaction temperature (20.28 K) at atmospheric pressure. This precooling stage is originally planned to be conducted by another magnetic refrigeration system called an Active Magnetic Refrigeration (AMR), which is not the topic of this paper.[15] Figure 1 shows this refrigerator condenses hydrogen gas directly on the surface of the magnetic material, subsequently liquid hydrogen drops downwards to a reservoir. The principle is equivalent to a thermo-siphon, a type of a heat pipe, and categorized into the heat transport regime making use of the gravity unlike the normal thermo-siphon which uses capillary phenomena for liquid circulation. As seen in Fig. 1, the hydrogen gas is liquefied directly on the magnetic material surface eliminating heat exchanger loss and increasing the efficiency.
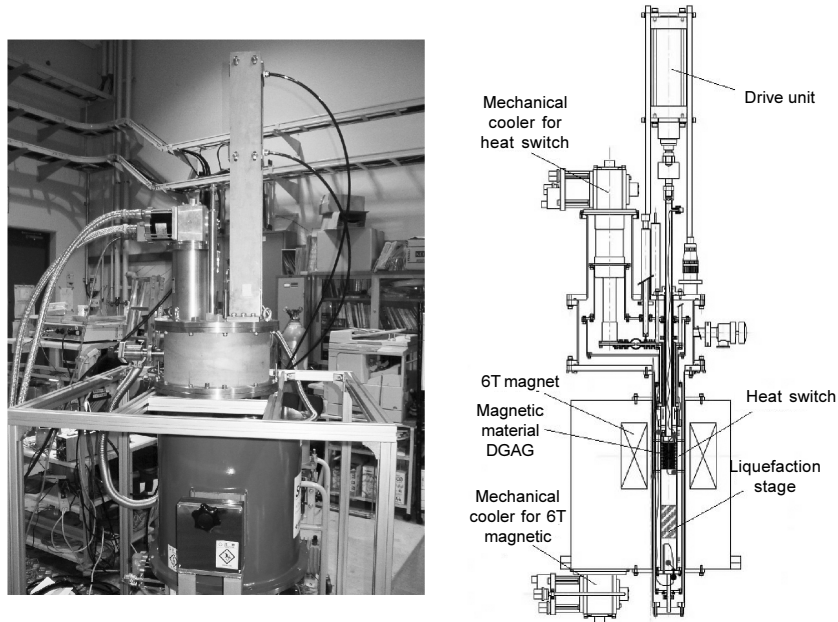
Hydrogen Magnetic Refrigerator

Figure 2 shows our magnetic refrigerator consisting of a magnetic refrigerant, a 6 Tesla superconducting magnet and a heat switch. The magnetic field applied to the magnetic refrigerant is varied by moving the refrigerant (0.28 kg of DGAG) by 15 cm in the magnet with a drive shaft connected to an air compressor. Since the superconducting magnet is a solenoid type of a magnet without a bucking coil, the magnetic field only reduces to 1T at 15 cm away from the magnet center. However, DGAG exhibits a large entropy change at a higher magnetic field and the 15 cm stroke shouldn't matter.

In Fig. 2, at the start of the cooling cycle, DGAG initially at the center of the magnet, starts to move downwards to a shaded area called the liquefaction stage and decreases its temperature by the magnetocaloric effect. Hydrogen gas filling the liquefaction stage starts liquefying when the DGAG temperature dips below the liquefaction temperature. After a certain period, DGAG starts to move back to the original magnet center and increases in temperature. Heat from DGAG is expelled at the magnet center with a gas-gap heat switch connected to a conventional Gifford-MacMahon (G-M) mechanical cryocooler. For our refrigerator, the operation frequency is adjustable from 0.01 Hz to 0.5 Hz, but a high
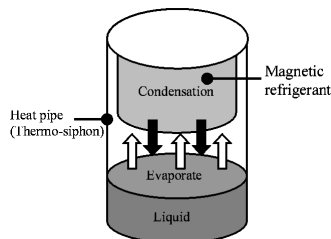
Figure 1. Liquefaction principal of our magnetic refrigerator based on thermo-siphon method.

Figure 2. A picture (left) and a drawing (right) of our magnetic refrigerator

power air compressor is needed for higher frequencies because it is difficult for the air compressor to recharge the air in time at higher frequencies.

As for a thermal aspect of the refrigerator, the drive shaft is a critical component because the top of the shaft is exposed to the room temperature and the bottom is at liquid hydrogen temperature, 20 K. In addition, the shaft brings shuttle heat transfer by moving up and down. In order to minimize the heat leak, the two different materials, stainless for the upper half shaft and FRP for the lower shaft, are used for the drive shaft because the upper shaft is closed up with the Wilson seal. The gas-gap heat switch is a hollow cylinder made of copper to surround the DGAG holder with a 1 mm clearance when the DGAG holder is at the magnet center. Generally, the performance of the gas-gap heat switch is determined by the heat transfer coefficient given below.

$$h = \lambda / d$$

(1)

where λ is the gas thermal conductivity, d is the gap width. It is seen that the heat transfer coefficient is inversely proportional to the gap.

MAGNETIC MATERIAL

Magnetic Property and Housing of Magnetic Material

Although metal compounds are used for general magnetic refrigeration, most metals don't satisfy the hydrogen resistance, one of the most important properties, because the hydrogen liquefies directly on the surface of the magnetic refrigerants. In this study, we have developed a new ceramic magnetic refrigerant, DGAG, to avoid this difficulty. We started with the DAG since it has a relatively large magnetocaloric effect around hydrogen boiling temperature and has been studied intensively for a long time. The reason for adding Gd is that garnets, including Gd, tend to be magnetically isotropic. The Gd ion is generally localized in the garnet crystal structure due to no LS coupling. In addition, adding the Gd ion increases the zero magnetic field entropy because of the large magnetic moment of the Gd ion; J=7/2. These are important factors to enhance the magnetocaloric effect. Fig. 3 shows the entropy diagram for the poly crystal 20% DGAG.

To maximize the surface area of the DGAG and for the hydrogen gas to flow without large pressure loss, the DGAG is formed in a slit shape as seen in Fig. 4. Thus, the whole DGAG holder consists of a
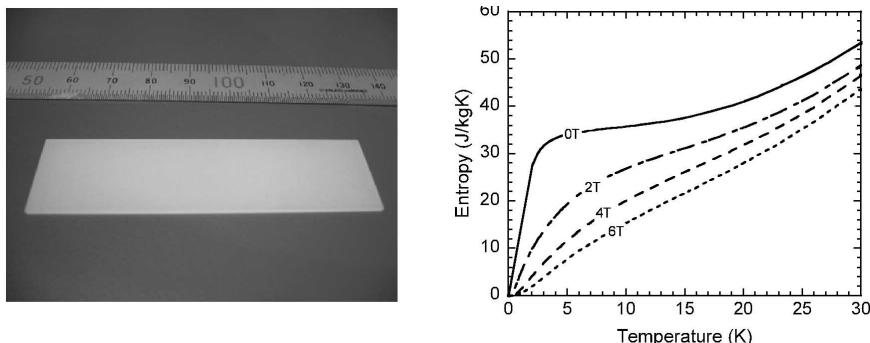
Figure 3. A picture (left) of the poly crystal 20%DGAG formed as a rectangular solid and its entropy diagram (right) at several magnetic fields.

copper hollow cylinder and rectangular solid DGAGs line up in parallel to each other with a gap of 1 mm. The holder is placed in parallel to the hydrogen flow direction. In addition, to minimize heat generation from eddy current in the copper cylinder when the magnetic field is changed, the copper cylinder is divided into 4 parts to prevent eddy current to circulate in the cylinder, and its thickness is reduced to 1 mm. Consequently, the heat generation was suppressed to 0.3 W at 20 K and at 0.01 Hz in the 6T magnetic field.

Magnetic Torque

The magnetic torque to the DGAG can be very large when the refrigerator operates at 6T. Since spins tend to line up in parallel to the applied magnetic field, DGAG is attracted to the magnet center. The magnetic torque is defined by

$$F = M \cdot \frac{\partial B}{\partial z}. \tag{2}$$

where M is magnetization, B is the applied magnetic field, z is the distance from the magnet center. A calculated magnetic torque to DGAG is shown in Fig. 5 with the magnetic field profile. The slope of the magnetic field depends on DGAG position, and the maximum magnetic torque was found to reach 1kN. This number, however, is acceptable for normal commercial air compressors. Furthermore, another calculation by the authors suggests that a twin or even multiple DGAG system will drastically reduce the single magnetic torque.[16] Since multiple systems can reduce the power input as well as the torque. This feature will be employed in a next system.
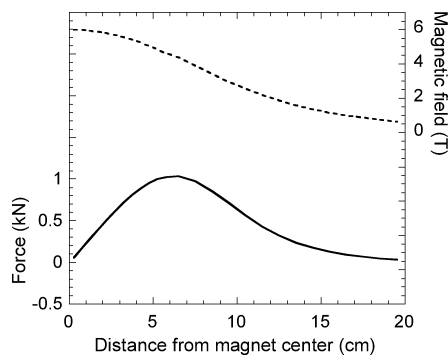
EXPERIMENT AND RESULTS

Preparation of Precooled Gas Hydrogen

There are two kinds of hydrogen gas states called ortho hydrogen and para hydrogen. In an equilibrium state at room temperature, the ratio of ortho H_2 and para H_2 is approximately 3:1. The ratio of para

Figure 4. A picture of DGAG holder from the top view (left) and a cross shot of its schematic drawing (right).

Figure 5. Magnetic field profile in 6 T superconducting magnet and corresponding magnetic torque on DGAG.

hydrogen increases when lowering the temperature and becomes almost 100% at the liquefaction temperature. At any temperature, the hydrogen at ortho- para ratio of 3:1 is called normal hydrogen (n-H_2). On the other hand, the hydrogen in an equilibrium state at a certain temperature is called equilibrium hydrogen (eH_2). Due to an energy gap between n-H_2 and e-H_2, the conversion heat from n-H_2 to e-H_2 exists. In experiments, e-H_2 is set to a temperature slightly above boiling point converting ortho to para so that the hydrogen doesn't boil off immediately after liquefaction. Since the conversion requires several days, a ferric oxide catalyst is used to speed up the conversion.

Preparation of Precooled Gas Hydrogen

Normally for liquefaction experiments, a liquid level detector is used to measure the amount of liquid. In our experiments, the hydrogen liquefaction is judged from the temperature variation with thermometers on DGAG due to the lack of an appropriate commercial level detector for our small experimental cell. Figure 6 shows DGAG temperature variation in e-H_2 during liquefaction process. Grey area indicates the demagnetizing process and the broken line is the hydrogen condensation temperature (boiling point) under corresponding saturated vapor pressure. It is seen in Fig. 6 that the DGAG temperature starts decreasing upon the onset of demagnetization at the point A due to the magnetocaloric effect, and ends decreasing at the end of the demagnetization at point C. In the demagnetization process, discontinuity in the temperature slope indicated by B is seen in Fig. 6. Since the DGAG temperature at this discontinuity coincides with the hydrogen condensation temperature indicated by the broken line in the Fig. 6, we conclude that the discontinuity point means the beginning of liquefaction. For a comparison, the DGAG temperature variation in n-H_2 when liquefaction doesn't occur with a similar condition is shown in Fig. 7. It is seen that there is a meaningful difference in the temperature change between the two cases because the gas state is closer to the adiabatic condition which creates larger ΔT than in the liquid state. In other words, when liquefaction, partly because the heat transfer coefficient becomes larger and because the cooling power is immediately
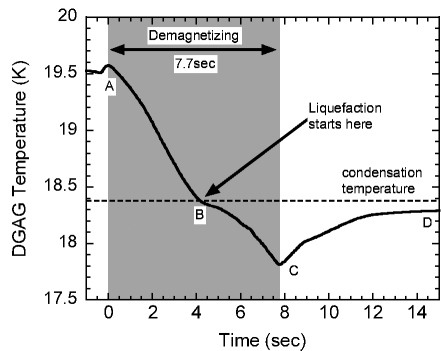
Figure 6. The temperature variation of the DGAG in the liquefaction process. The magnetic field is varied for 7.7 seconds in a gray area. A discontinuity point indicates liquefaction starts.
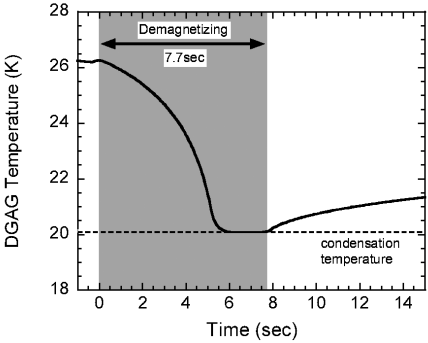
Figure 7. The temperature variation of DGAG in n-H_2 atmosphere in the liquefaction process at the speed of 7.7 sec demagnetization. Liquefaction doesn't occur because the conversion heat is large.
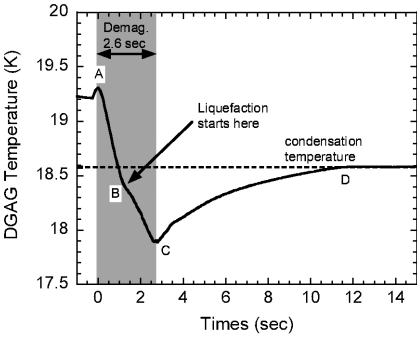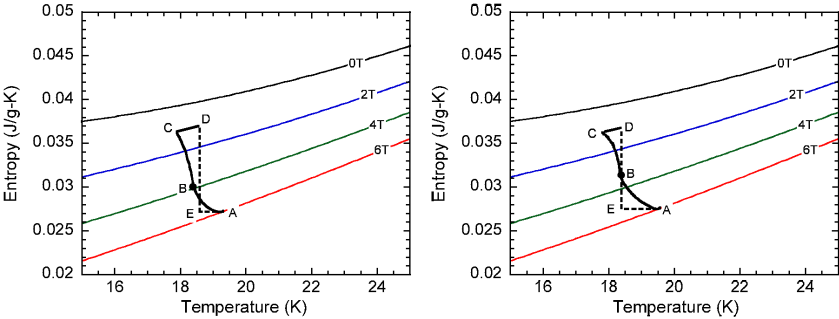

Figure 8. The temperature variation of DGAG in the liquefaction process at the speed of 2.6 sec demagnetization. It is seen that the hydrogen is supercooled due to the fast demagnetization.

consumed by the growth of liquid film forming on the surface of the DGAG, ΔT of the DGAG becomes relatively smaller.

Figure 8 shows the DGAG temperature variation at a different demagnetization speed. In Fig. 8, a discontinuity point B is seen to come to below the condensation temperature. This is because hydrogen undergoes supercooling state due to too fast demagnetization. In addition, it is also seen in Fig. 8 that the DGAG temperature quickly comes up to its condensation temperature.

In order to estimate the efficiency and the cooling power, the temperature variation in Figs. 6 and 8 are converted into the entropy diagrams shown in Figs. 9(a) and (b), respectively. The entropy changes of DGAG at several magnetic fields are also shown in Figs. 9. Both liquefaction processes in Figs. 9 are indicated by solid lines A-B-C-D corresponding to the points in Figs. 6 and 8. A dotted line A-E-D is the

Figure 9. The entropy diagrams converted from the DGAG temperature variation and position. A left figure(a) is converted from Fig.8 at the speed of 2.6 demagnetization A right figure(b) is converted from the temperature in Fig. 6.
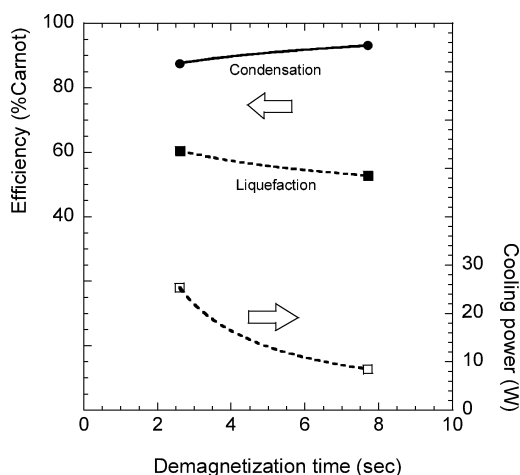
Figure 10. The efficiency in condensation and liquefaction process estimated from the entropy diagram in Figure 9. The cooling power in liquefaction process also calculated and shown in the figure.

demagnetization process of the ideal Carnot cycle with the isothermal process at its condensation temperature. It is seen in Figs. 9 that both liquefaction processes deviate from the Carnot processes. Normally, the demagnetization process in the Carnot cycle consists of an adiabatic process A-E and an isothermal process E-D, but it is difficult to apply this analogy to the liquefaction process in our magnetic refrigerator. Therefore, for the clarity of discussion, we define a "non-condensation" process A-B as a period from the beginning point of demagnetization (A) to the beginning point of liquefaction (B) which corresponds to the adiabatic process in the Carnot cycle. In the same manner, a "condensation" process B-C-D is defined as a period from the beginning point of liquefaction (B) to the end point of liquefaction (D) via (C).

In a comparison of Figs. 9(a) and (b), the deviation of non-condensation process A-B in the real cycle from the Carnot cycle seems to decrease with cycle speed. This result reflects a fact that the efficiency in this process increases with the cycle speed. The non-condensation process is equivalent to weakly "ON" state of a heat switch due to the heat transfer from warm surrounding hydrogen gas to the DGAG. Thus, the amount of the heat transfer that is to say the inefficiency is thought to decrease with the cycle speed. On the contrary, it is reasonable that the deviation of the condensation process B-C-D from the Carnot increases with the cycle speed.

Finally, the efficiency and the cooling power of our magnetic refrigerator of the liquefaction process are estimated and shown in Fig. 10. It was found that the condensation efficiency reaches 90% Carnot and the liquefaction efficiency reaches greater than of 50% of the Carnot efficiency. The liquefaction power is found to decrease with demagnetization time and the maximum power was 25.3 W.

SUMMARY

We have built the magnetic refrigerator and successfully liquefied hydrogen. It was found that the condensation efficiency accomplished 90% Carnot and the liquefaction power was 25.3 W in hydrogen liquefaction process at atmospheric pressure. In a subsequent paper, we plan to follow the whole cooling cycle to see the refrigerator performance. In addition, development of a hydrogen level detector to directly measure the amount of the liquid is under way.

REFERENCES

1. Baker, C. B., "A Study of the Efficiency of Hydrogen Liquefaction," *International Journal of Hydrogen Energy*, Vol.3, (1978), pp.321-334.

2. Utaki, T., "Efficiency Evaluation of Magnetic Refrigerators for Hydrogen Liquefaction by Numerical Simulation," *Master Thesis*, Osaka University, (2006).

3. Numazawa, T., Kimura, H., Sato M. and Maeda H., "Carnot Magnetic Refrigerator Operating between 1.4 and 10 K," *Cryogenics*, Vol. 33, Issue: 5 (May 1993), pp. 547-554.

4. Debye, P., *Annalen der. Physik,* vol. 81, (1926), p.1154.

5. Giauque, W.F., *Journal of American Chemistry Society*, Vol. 49, (1927) p. 1870.

6. Pecharsky, V.K. and Gschneider Jr., K.A., "Tunable Magnetic Regenerator Alloys with a Giant Magnetocaloric Effect for Magnetic Refrigeration from 20 K to 290 K," *Applied Physics Letter*, Vol.70, No. 24 (1997), p. 16.

7. Yamamoto, T.A., Nakagawa, T., Sako, K., Arakawa, T. and Nitani, H., "Magnetocaloric Effect of Rare Earth Mono-Nitrudes, TbN and HoN," *Journal of Alloy and Compound*, Vol. 376 (2004), pp. 17-22.

8. Nakagawa, T., Sako, K., Arakawa, T. and Yamamoto, T.A., "Magnetocaloric Effect of Mono-Nitride containing Gdolinium and Dysprosium GdxDy1-xN," *Journal of Alloy and Compounds*, Vol. 364 (2004), pp. 53-58.

9. Wada, H., Tomekawa, S. and Shiga, M., "Magnetocaloric Properties of a First-Order Magnetic Transition System $ErCo_2$," *Cryogenics*, Vol. 39, Issue: 11 (November 1999), pp. 915-919.

10. X.X.Zhang, J.Tejada, Y.Xin, G.Sun, K.W.Wong and X.Bohigas, "Magnetcaloric Efect in $La_{0.67}Ca_{0.33}MnO$ and $La_{0.60}Y_{0.07}Ca_{0.33}MnO$ Bulk Materials," *Appl. Phys. Lett*. **69** (23), 2 December 1996.

11. Numazawa, T., Kamiya, K., Okano, T. and Matsumoto, K., "Magnetocaloric Effect in $(Dy_xGd_{1-x})_3Ga_5O_{12}$ for Adiabatic Demagnetization Refrigeration," *Physica B*, vol. 329-333, (2003), pp. 1656-1657.

12. Barclay, J.A. and Steyert, W.A., "Materials for magnetic refrigeration between 2 K and 20 K," *Cryogenics*, Vol. 22, Issue: 2 (February 1982), pp. 73-80.

13. Ohira, K., Matsuo, S., Furumoto, H., "The Characteristics of Magnetic Refrigeration Operating at the Temperature of 20 K," *Proceedings of the 16th International Cryogenic Engineering Conference* (1996), pp. 403-406.

14. Kamiya, K., "Design and Build of Magnetic Refrigerator for Hydrogen Liquification", *Adv. in Cryogenic Engineering*, Vol. 51B, Amer. Institute of Physics, Melville, NY (2004), pp. 591-597.

15. Engelbrecht, K.L., "A Numerical Model of an Active Magnetic Regenerator Refrigeration System," *Master Thesis*, University of Wisconsin, (2004).